

Gas source molecular beam epitaxy of FeSi₂/Si(111) heterostructures

H. Ch. Schäfer, B. Rösen, H. Moritz, A. Rizzi,^{a)} B. Lengeler, and H. Lüth
*Institut für Schicht- und Ionentechnik, Forschungszentrum Jülich, Postfach 1913, D-5170
 Jülich, Germany*

D. Gerthsen
Institut für Festkörperforschung, Forschungszentrum Jülich, Postfach 1913, D-5170 Jülich, Germany

(Received 10 September 1992; accepted for publication 8 March 1993)

Epitaxial iron disilicide thin layers have been grown on silicon by gas source molecular beam epitaxy (GSMBE) in the temperature range 450–550 °C. Fe(CO)₅ and SiH₄ are used as sources for the silicide growth on a heated Si(111) surface. The growth phases are characterized *in situ* by means of high-resolution electron energy loss spectroscopy, ultraviolet and x-ray photoelectron spectroscopies. The formation of an epitaxial metallic γ -FeSi₂ layer at the interface with the silicon substrate is revealed and no complete relaxation of this strained metastable interface layer is observed, as the growth proceeds with the semiconducting equilibrium β -FeSi₂ phase. The coexistence in the GSMBE grown heterostructures of the metallic (CaF₂) and semiconducting (orthorhombic) FeSi₂ structures is confirmed by cross-section transmission electron microscopy.

Continuous effort is put into the research of possible new candidate materials for developing optoelectronic devices based on silicon. SiGe/Si as well as GaAs/Si heterostructures have received much attention and recently some work has been going on concerning the growth and characterization of β -FeSi₂ on silicon. This low temperature phase of iron disilicide crystallizes in an orthorhombic structure and has a semiconducting character with an energy gap of about 0.9 eV.¹

The epitaxial growth of very thin β -FeSi₂ layers on Si(111) has first been achieved under UHV conditions by solid phase epitaxy (SPE) in which iron is deposited from a solid source on the clean silicon surface and annealing promotes the reaction with the Si atoms from the substrate.^{2–5} Common features of these types of samples are a nonuniform morphology and a significant surface roughness, as shown by scanning tunneling microscopy.⁶

Onda *et al.*⁷ have grown FeSi₂/Si(111) heterostructures by molecular beam epitaxy (MBE) and they found a new metastable phase for this material on Si(111); this γ -FeSi₂ has a cubic fluorite structure, is metallic, and is completely analogous to NiSi₂ and CoSi₂ grown epitaxially on Si(111). Christensen⁸ reported on this fluorite structure for FeSi₂ as a hypothetical phase in his calculations and because of a high density of states at the Fermi level this metallic phase undergoes a structural as well as an electronic transition toward a lower energy configuration represented by the orthorhombic semiconducting β -FeSi₂. The formation of γ -FeSi₂ on Si(111) was even observed with solid phase reaction methods, but limited to smaller thicknesses.^{3,5}

In this letter, the growth of FeSi₂/Si(111) heterostructures by gas source molecular beam epitaxy (GSMBE) is reported and the coexistence of both metallic and semiconducting disilicide phases is observed and discussed.

GSMBE was first developed for III-V epitaxy combin-

ing the advantages of continuous performance and self-adjusting stoichiometry provided by the reaction of the components at the sample surface. This technique provides defect-free surfaces and selective growth is possible; it therefore represents a very powerful growth method for LSI. Only recently was GSMBE applied to silicon and SiGe/Si epitaxy, confirming the high quality of the layers grown in this way.^{9,10}

The experimental setup consists of three UHV chambers connected in series; a load-lock entry allows rapid insertion of the sample into the growth unit. The first analysis chamber is equipped with a high resolution electron energy loss (HREEL) spectrometer (one stage monochromator and analyzer). The second analysis chamber is devoted to ultraviolet (UPS) and monochromatized x-ray photoelectron spectroscopy (XPS).

Si(111) *n*-type (P doped, 1–10 Ω cm) wafers (5 \times 10 mm²) are used as substrates; they are chemically treated before insertion into the UHV chamber. Annealing at 820 °C for 5 min causes desorption of the surface oxide and provides a clean Si(111)(7 \times 7) surface as checked by HREELS and UPS.

Iron pentacarbonyl [Fe(CO)₅] and silane (SiH₄) are used as beam sources and separately injected into the growth chamber through glass capillary arrays focused onto the sample surface. The gas flow, controlled by Baratron valves, is maintained at a constant ratio of 2:5, respectively, for the Fe and Si components. The gas pressure at the inlet valves is 1 \times 10⁻² Torr and the background pressure in the chamber during the growth is 8 \times 10⁻⁶ Torr. A cryoshield, surrounding the gas sources on the UHV side, is maintained at low temperature by continuous liquid nitrogen flow during the growth process. The reactant gases are decomposed on the surface, which is heated at *T* = 450–550 °C by means of direct current flow through the sample. No traces of carbon incorporation in the as-grown layers are revealed within the sensitivity of the employed *in situ* techniques.

Figure 1 shows a sequence of normalized UPS (a) and

^{a)}Permanent address: Dipartimento di Fisica, Università di Modena, via Campi 213/A, I-41100 Modena, Italy.

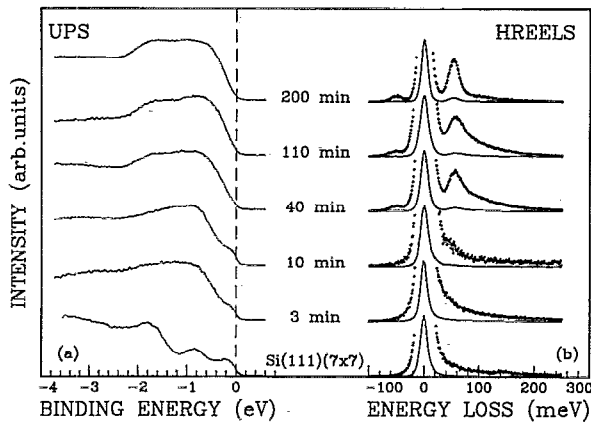


FIG. 1. (a) UPS valence-band spectra measured at room temperature on a $\text{FeSi}_2/\text{Si}(111)$ heterostructure after successive growth steps at 550°C . The indicated time for each step is the total exposure time (growth rate is about $3 \text{ \AA}/\text{min}$). Photon energy is 21.2 eV ; the Fermi level position is indicated by the vertical dashed line at zero binding energy. (b) High-resolution electron energy loss spectra taken after the same growth steps as in (a) with a primary beam energy of 7 eV under specular reflection ($\theta=57^\circ$). The dotted curves correspond to a magnification by a factor of 10.

HREELS (b) spectra taken on the clean $\text{Si}(111)(7\times 7)$ surface and after increasing exposures within one and the same growth process at a substrate temperature of 550°C ; the growth rate was $\sim 3 \text{ \AA}/\text{min}$. The spectra were taken at room temperature after interrupting the growth. After 3 and 10 min growth the loss spectra are structureless, as for the clean (7×7) surface, the quasielastic peak has broadened and a clear asymmetric background extends up to some hundreds of meV on the loss side. The UPS spectra at this stage of the growth show a clear Fermi edge and a major emission structure extending up to $\sim 2.2 \text{ eV}$ binding energy. After the next growth step, both spectra clearly change. A loss structure at 50 meV emerges out of the background and a corresponding peak is visible on the gain side. In UPS at the top of the valence band a broad structure occurs between 0.6 and 2.4 eV and the emission at the Fermi energy is strongly reduced. From this point on the UPS spectra do not change anymore whereas in HREELS the loss peak at 50 meV becomes more and more pronounced with respect to the background and the quasielastic peak gradually narrows.

HREELS and UPS show unambiguously the formation of two different phases during the growth. A quantitative analysis of the $\text{Si}(2p)$ and $\text{Fe}(3d)$ core levels as measured by XPS gives a FeSi_2 stoichiometry for both phases. At the beginning a metallic layer is grown on silicon as shown by the clear Fermi edge in the UPS spectra together with the structureless HREEL spectra, as in the case of the "metallic" (7×7) silicon surface reconstruction. According to our previous UPS and HREELS experiments on $\text{FeSi}_2/\text{Si}(111)$ heterostructures grown by SPE,⁵ the growth of a $\gamma\text{-FeSi}_2$ layer is assumed at this first stage of the GSMBE. A simulation of the HREEL spectrum [$\gamma\text{-FeSi}_2$ (9 \AA)/ $\text{Si}(111)$, not shown here] agrees well with the experiment, reproducing the observed broadening of the elastic peak and the loss background. In the framework

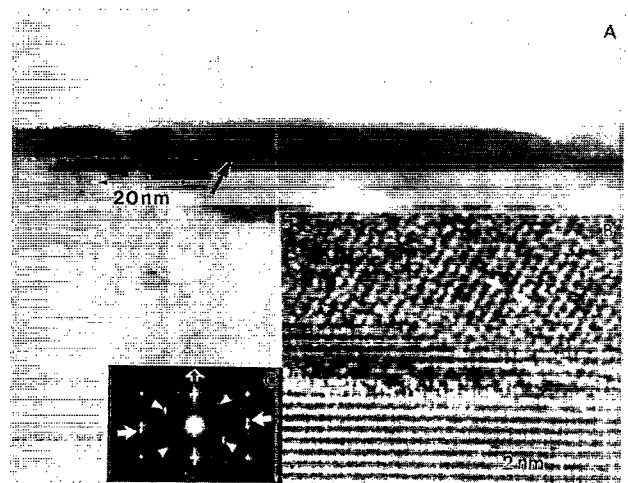


FIG. 2. (a) A $\langle 112 \rangle$ cross-section image of FeSi_2 on $\text{Si}(111)$. The arrow points to the sharp interface between the FeSi_2 and the substrate. There, the narrow dark line extending all over the sample is attributed to metallic $\gamma\text{-FeSi}_2$. (b) A $\langle 112 \rangle$ high-resolution cross-section image of the interface region. The arrows indicate the spacing of the $\beta\text{-FeSi}_2$ (202) or (220) planes, respectively. (c) Optical diffractogram obtained by a Fourier transform of the area shown in (b). Triangular symbols mark the $\beta\text{-FeSi}_2$ (202) or (220) planes. The closed arrows mark the $\beta\text{-FeSi}_2$ (040) or (004) planes. The open arrow points into the growth direction.

of the dielectric theory such a spectrum is due to multiple excitation of low energy plasmon modes arising from the coupling of interface modes in a very thin ($\sim 10 \text{ \AA}$) metallic layer on top of a semiconductor. After 40 min of growth the HREEL spectrum shows the excitation of a surface phonon characteristic of the semiconducting $\beta\text{-FeSi}_2$.^{4,5} Nevertheless the persisting loss background is an indication that the $\gamma\text{-FeSi}_2$ layer remains stabilized at the interface. The shape of the UPS spectrum is that of the orthorhombic semiconducting phase^{5,8,11} with negligible density of states at the Fermi level. Due to the high surface sensitivity of UPS, no contribution from the buried $\gamma\text{-FeSi}_2$ layer is revealed. As growth proceeds the relative weight of the two phases in the loss spectra produces a more and more $\beta\text{-FeSi}_2$ -like spectrum, as expected from the probing depth of the experiment (some hundreds of \AA). The combined spectroscopic investigation, HREELS, and UPS, thus indicates at the beginning of the GSMBE the formation of a continuous and very thin metallic $\gamma\text{-FeSi}_2$ layer followed by the growth of the semiconducting $\beta\text{-FeSi}_2$ phase on top. The reported sequences of phase growth has been observed in the temperature range $450\text{--}550^\circ\text{C}$ and confirmed by transmission electron microscopy (TEM).

Results of a TEM analysis on a sample grown by GSMBE at $T=500^\circ\text{C}$ are shown in Fig. 2. The overview image (A) shows for the grown layer homogeneous thickness ($8\text{--}10 \text{ nm}$) and a sharp interface with the $\text{Si}(111)$ substrate; further, crystalline domains with typical lateral sizes ranging from 100 nm up to $1 \mu\text{m}$ can be identified. A high-resolution cross-section image of the interface region is displayed in Fig. 2(b). The electron beam was parallel to a $\text{Si}\langle 112 \rangle$ zone axis. The uppermost eight (111) planes of the substrate and, perpendicular to them, the $\text{Si}(\bar{2},2,0)$ planes, are clearly resolved. Above, the resolution is lost

for the thickness of about two Si(111) layers which is indicative of local strain-relief relaxation at the interface¹² [see also the streaks through Si reflections in Fig. 2(c)]. On top of that, two to three layers are observed which exhibit the same lattice spacings as the silicon. However, this layer appears considerably darker than the silicon substrate. A thin layer of dark contrast can also be recognized, marked by the arrow, in the overview image (A). According to the previous spectroscopic analysis, the growth of strained γ -FeSi₂ in a $\langle 112 \rangle$ zone-axis orientation is assumed. Its CaF₂ structure exhibits the same symmetry as the Si and, according to theory,⁸ almost the same lattice parameter ($a=0.5389$ nm). High-resolution image simulations which will be reported in a further publication support this hypothesis.

On top of the γ -FeSi₂, β -FeSi₂ observed. Only one set of lattice planes is resolved [β -FeSi₂(202) or (220)] because the β -FeSi₂ is not oriented with a low index zone axis parallel to the electron beam. However, the optical diffractogram (corresponding to a Fourier transform of the image) taken from the region shown in part (B) yields more information about the epitaxy. The reflections marked by the triangular symbols correspond to the β -FeSi₂ (220) and (202) planes. The big arrow points to reflections induced by β -FeSi₂ (040) or (004). The epitaxial relationship between the β -FeSi₂ and the substrate can directly be deduced. In addition to what is reported for SPE-grown β -FeSi₂ on Si(111),² even β -FeSi₂(100) oriented almost parallel (slightly tilted) to the Si(111) is observed in our case. The azimuthal orientation for this epitaxy corresponds to β -FeSi₂[040]|| Si $\langle 220 \rangle$ or β -FeSi₂[004]|| Si $\langle 220 \rangle$.

In conclusion, the growth of epitaxial FeSi₂/Si(111) heterostructures has been achieved in the temperature range $T=450$ – 550 °C by gas source MBE using Fe(CO)₅ and SiH₄ as source molecules. The morphology of the as-grown layers shows the formation of crystalline domains

with a very smooth surface together with a very sharp interface with the substrate. A combined HREELS and UPS *in situ* analysis reveals at the Si(111) interface the formation of a very thin metallic γ -FeSi₂ strained layer which is preserved during the subsequent growth of β -FeSi₂, as is also confirmed by TEM.

This particular type of growth can be explained in terms of a total energy consideration. At the beginning, depending on the temperature and growth process, the growth of the strained γ phase is energetically favored compared to the equilibrium β phase. At a certain point the strain energy becomes too high and the stable semiconducting β phase begins to grow. A relaxation of the γ layer would imply a higher total energy and the fact that FeSi₂ on Si(111) can be stabilized at low temperature in its two polytypes (metallic CaF₂ and semiconducting orthorhombic structures) is the reason for this interesting type of growth.

¹U. Birkholz and J. Schelm, Phys. Status Solidi 27, 413 (1968).

²J. Derrien, J. Chevrier, V. Le Thanh, and J. E. Mahan, Appl. Surf. Sci. 56–58, 382 (1992).

³J. Chevrier, V. Le Thanh, S. Nitsche, and J. Derrien, Appl. Surf. Sci. 56–58, 438 (1992).

⁴A. Rizzi, H. Moritz, and H. Lüth, J. Vac. Sci. Technol. A 9, 912 (1991).

⁵H. Moritz, B. Rösen, S. Popović, A. Rizzi, and H. Lüth, J. Vac. Sci. Technol. B 10, 1704 (1992).

⁶J. de la Figuera, A. L. Vázquez de Parga, J. Alvarez, J. Ibáñez, C. Ocal, and R. Miranda, Surf. Sci. 264, 45 (1992).

⁷N. Onda, J. Henz, E. Müller, K. A. Mäder, and H. von Känel, Appl. Surf. Sci. 56–58, 421 (1992); N. Onda, J. Henz, E. Müller, H. von Känel, C. Schwarz, and R. E. Pixley, Helv. Phys. Acta 64, 197 (1991).

⁸N. E. Christensen, Phys. Rev. B 42, 7148 (1990).

⁹H. Hirayama, T. Tatsumi, A. Ogura, and N. Aizaki, Appl. Phys. Lett. 51, 2213 (1987).

¹⁰A. Yamada, M. Tanda, F. Kato, M. Konagai, and K. Takahashi, J. Appl. Phys. 69, 1008 (1991).

¹¹J. Alvarez, J. J. Hinarejos, E. G. Michel, G. R. Castro, and R. Miranda, Phys. Rev. B 45, 14042 (1992).

¹²R. G. Dandrea and C. B. Duke, Phys. Rev. B 45, 14065 (1992).